ELSEVIER

Thermochimica Acta 312 (1998) 115–124

thermochimica acta

Energetics of H_2 and O_2 adsorption on Ir/γ-Al_2O_3 and Ir/SiO_2 catalysts. Dependence on support and on metal particle size

J.M. Guil*, A. Pérez Masiá, A. Ruiz Paniego, J.M. Trejo Menayo[1]

Instituto de Química Física "Rocasolano", CSIC. Serrano, 119, 28006-Madrid, Spain

Abstract

The adsorption of hydrogen and oxygen on Ir/SiO_2 and Ir/Al_2O_3 catalysts of various metallic percentages and different metal particle sizes has been studied by adsorption microcalorimetry. The hydrogen adsorption stoichiometries lay between 1.1 and 2.4, depending on the support and on degree of dispersion. The variation of hydrogen adsorption heat with amount adsorbed revealed significant differences in surface heterogeneity between the various samples. The dependence of hydrogen adsorption stoichiometry and differential heat of adsorption vs. coverage curves on support and on particle size may be related to crystallite size and shape, and to differences in metal-support interaction. On the contrary, oxygen adsorption stoichiometries and differential heat of adsorption vs. coverage curves were very similar for all samples. The amount of oxygen adsorbed at the completion of the monolayer, clearly identified in the differential calorimetric isotherms, coincided with the amount of superficial iridium as determined by a volumetric method. © 1998 Elsevier Science B.V.

Keywords: Adsorption; Iridium; Microcalorimetry; Supported catalysts

1. Introduction

Iridium has been usually included in systematic studies on the catalytic applications of group VIII transition metals. It has been investigated as a catalyst for various chemical processes utilizing its specific activity: hydrogenation, hydrocarbon activation, isomerization, hydrocarbon synthesis, partial oxidation of methane, water–gas shift reaction, either alone [1–9], or as bimetallic catalysts [10–12]. Presently, papers appear regularly in which iridium has become the particular objective of research. The interest is focussed on the ability of iridium to activate hydrocarbons by C–C bond cleavage upon adsorption [13,14], and the extension of its possibilities as catalyst when iridium is dispersed as clusters [6–8,15].

We have already established a method for determining the amount of surface iridium on supported catalysts [16,17]. In these studies, it was found that the chemisorptive behaviour of hydrogen and oxygen depended on the support used as well as on the iridium particle size. As an extension of this research, it was considered interesting to investigate the energetics of these adsorption systems by means of adsorption microcalorimetry. It is the main objective of the present work to afford information on the energetics of oxygen and hydrogen/iridium-supported catalyst systems that can have application in the study of some of the aforementioned catalytic reactions. A second goal was to validate our volumetric method of determining iridium dispersion while taking advantage of the detailed information supplied by microcalorimetric measurements.

*Corresponding author. Fax: 34 1 564 24 31; E-mail: rocguil@iqfr.csic.es

[1]Present address: Repsol Petróleo, S.A. Embajadores, 183, 28045-Madrid, Spain.

PII S0040-6031(97)00445-0

2. Experimental

2.1. Materials

Hydrogen and oxygen (Sociedad Española del Oxígeno, Spain), 99.995% pure, were used as adsorbates. Hydrogen was introduced into the apparatus through a palladium thimble heated to ca. 600 K. Oxygen was purified inside the apparatus by successive freeze–thaw cycles.

Samples of supported iridium were prepared by the incipient wetness impregnation method, using a solution of hexachloroiridic acid (Alfa Ventron Inorganics, Germany) [16,17]. A silica gel (BASF D-11-11, BET specific surface area 128 $m^2\ g^{-1}$) and a γ-alumina (Girdler T-126, BET specific surface area 149 $m^2\ g^{-1}$) were employed as supports. They had previously been treated in air at 973 K for 4 h. The impregnated samples were reduced in a hydrogen flow (60 $cm^3\ min^{-1}$) under the following temperature programme:

$$T_{room} \xrightarrow{1\,h} 373\,K(1\,h) \xrightarrow{1\,h} 473\,K(2\,h) \xrightarrow{2\,h} 723\,K(2\,h)$$

Sintered samples were prepared from the same reduced batch. They were kept in air at room temperature for 10 min so as to facilitate sintering, outgassed at the same temperature, and heated under vacuum for different times and temperatures.

The amount of surface iridium, n_{sf}(Ir), was determined by oxygen adsorption as described elsewhere [16,17]. Table 1 summarizes the characteristics of all the samples used (Col. 1). The time and temperature applied to produce the two sintered Ir/γ-Al_2O_3 2.5% samples are presented in the last two columns.

2.2. Adsorption volumetry and microcalorimetry

In order to obtain differential heats of adsorption as a function of coverage, the amount adsorbed for each dose and the corresponding heat evolved must be determined simultaneously. For this purpose, measurements were performed in a heat-flux microcalorimeter coupled to a volumetric apparatus, as described below.

Measurement of amounts adsorbed were performed in a conventional volumetric apparatus as described elsewhere [16,17]. The apparatus used in this work had twin cells, measurement and reference, positioned inside the two wells of the microcalorimeter. The reproducibility of measurements of the amount adsorbed was always better than 0.2 μmol.

Microcalorimetric measurements were carried out in a heat-flux microcalorimeter of the Tian–Calvet type (SETARAM, "low-temperature" model, France). It had two measurement wells for sample and reference cells provided with twin thermopiles, coupled in opposition so as to automatically balance out any spurious thermal effect. Inside these were placed the two matched cells of the volumetric apparatus. Adsorption experiments could be done by introducing gas either only into the adsorption cell or into both cells.

The measurement wells were hermetically isolated from the atmosphere which allowed control of pressure and the type of gas surrounding the two cells. To

Table 1
Characteristics of the catalyst samples

	Ir [a]/ %	n_{tot}(Ir) [a,c]/ (μmol g^{-1})	n_{sf}(Ir) [a,c]/ (μmol g^{-1})	l_c [d]/ nm	Sintering conditions	
					T/ K	*t*/ h
Ir/SiO_2 5%	5.45	283.5	95	2.8		
Ir/SiO_2 0.5%	0.54	28.1	7.5	3.5		
Ir/Al_2O_3 2.5%–1.1 and 2.5%–1.2	2.74	142.5	81	1.6		
Ir/Al_2O_3 2.5%–2.1	2.64	137.6	24.2	5.3	783	1
Ir/Al_2O_3 2.5%–2.2	2.64	137.6	11.6	10.8	829	2

[a] Referred to weight of catalyst dried under vacuum at 700 K.
[b] n_{tot}=total.
[c] n_{sf}=surface.
[d] Metallic particle size, assuming cubes standing on a face.

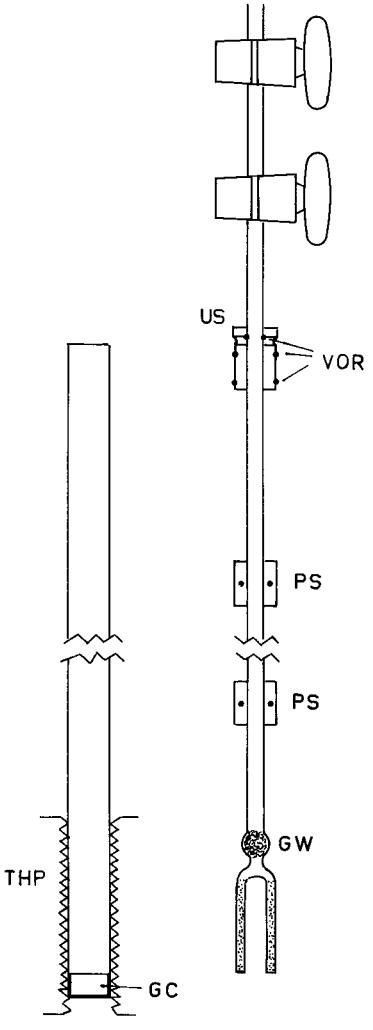

Fig. 1. Adsorption cell: US, upper stopper; VOR, Viton O-rings; PS, P.T.F.E. shields; GW, glass wool; GC, glass cylinder; and THP, thermopiles.

that end, a metallic stopper was fitted to the upper outlet of each calorimeter well and also to the corresponding cell glass tubing by Viton O-rings (Fig. 1). The cells fitted closely inside the respective calorimeter well. The catalyst was held near the outer wall of the cell by an inner glass tube (Fig. 1). Obviously, for obtaining maximum sensibility, the heat losses (i.e. heat not passing through the thermopiles) must be minimized. Special care was taken to prevent convection heat losses: two P.T.F.E. cylinders avoided convection outside the cell; and a glass wool plug hindered convection inside the cell (Fig. 1).

The limit of detection of the microcalorimeter was ≈0.5 mJ or 2 μW. Calibration of the heat/voltage constant of the microcalorimeter was accomplished by the Joule effect. The volume fraction of the cells lying within the thermopiles, V^{g}, necessary to calculate the so-called compression work, was determined by measuring the heat evolved in helium expansions. Reproducibility of the calorimetric measurements, estimated from the mean deviation of a series of helium expansion experiments, was ≈2 mJ.

With this setup, the increment of amount adsorbed, Δn^{σ}, the isothermal heat of adsorption, q_{th}, and the equilibrium pressure, p, could be measured simultaneously. The volumetric n^{σ} vs. p, and differential calorimetric, q_{th} vs. n^{σ}, isotherms were obtained from them. Although the use of a thermodynamic quantity, namely the differential molar energy of adsorption – change of internal energy – is recommended [18,19], in this work the differential molar enthalpy of adsorption, formerly called isosteric heat of adsorption $q^{st,\sigma}$, will be used instead because of its widespread use in data obtained both, by calorimetry and from adsorption isotherms. We have followed the calorimetric sign criterion (positive energetic quantity for an exothermic process).

2.3. Procedures

Once introduced into the cell, each sample was reduced in a static hydrogen atmosphere, following the same temperature programme used for reduction of the impregnated sample, but up to 700 K. The treatment was repeated every time the catalyst had been in contact with oxygen. Before each experiment, the sample was outgassed overnight at 673 K under a vacuum better than 1 mPa. The pretreatment was performed outside the calorimeter after which the cell was cut and joined to the system by glass blowing. Two high-vacuum greased stopcocks, placed in series (Fig. 1), ensured that the cell remained under vacuum during these operations.

Isotherms were obtained by successive additions of gas. The amount adsorbed and the heat evolved were measured simultaneously. Some readsorption isotherms were measured after outgassing at the same temperature of adsorption experiments for 15 min. All experiments were carried out at 315 K.

The adsorption on the support was taken into account. Both, the amount adsorbed and the heat evolved were determined by performing identical experiments on the silica and on the alumina supports [20], under the same conditions used for the iridium-supported samples. Substraction of these amounts allowed us to calculate the amount adsorbed and the adsorption heat on the metal. In a second method, an amount of support equal to that in the catalyst sample was introduced into the reference cell to automatically discount the adsorption on the support and to obtain $q^{st,\sigma}$ directly [21]. An inert solid was also introduced to make equal both V^g volumes. The two methods coincided and, consequently, only one cell was customarily used.

In the following, the net amount of adsorbate on iridium is expressed as micromoles of hydrogen or oxygen atoms per gram of catalyst dried in vacuum at 700 K, since it has been proved that these adsorbates are present as atoms on the iridium surface [17].

3. Results

3.1. Ir/SiO_2

Volumetric isotherms of *hydrogen adsorption* on the two Ir/SiO_2 samples are shown in Fig. 2(a). They are plotted as the ratio of amount of hydrogen atoms adsorbed to the amount of superficial iridium atoms, $n^{\sigma}(H)/n_{sf}(Ir)$, abbreviated as H^{σ}/Ir_{sf}, vs. pressure. Most adsorption occurred instantaneously at undetectable low equilibrium pressures. A knee with slower adsorption rates followed at $H^{\sigma}/Ir_{sf}\approx 1$. At higher pressures, there were small uptake increases in an activated adsorption process that did not reach equilibrium. This final part was somewhat different in different experiments. The readsorption isotherm is parallel to, but at a lower position than, the isotherm on the clean sample.

Differential calorimetric isotherms, $q^{st,\sigma}-n^{\sigma}$, on the two Ir/SiO_2 samples are coincident (Fig. 2(b)). The same results were obtained with the two methods mentioned in the previous section which proves their validity.

The heat of adsorption decreased monotonously with coverage. The slope decreases slightly at ca. $H^{\sigma}/Ir_{sf}=0.5$. An abrupt fall of the isosteric heat at

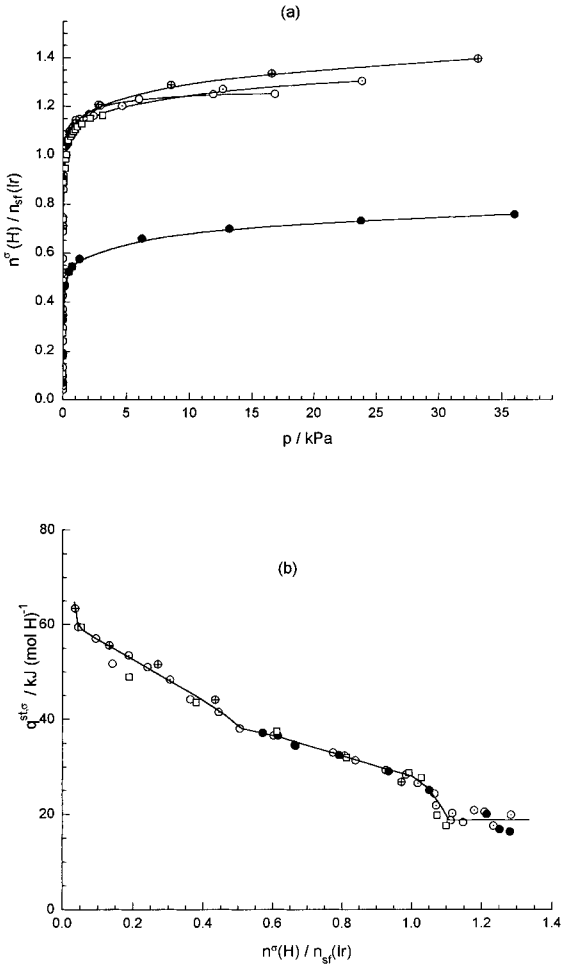

Fig. 2. (a) Volumetric and (b) differential calorimetric isotherms of hydrogen adsorption on Ir/SiO_2 samples at 315 K. Samples: 5%, ○, ⊕, ● (1 cell), ⊙ (2 cells); 0.5%, □ (2 cells). Filled symbols, readsorption experiments.

$H^{\sigma}/Ir_{sf}=1.1$ leads to a plateau at $q^{st,\sigma}\approx 17$–18 kJ (mol $H)^{-1}$. The experimental scattering is higher in this zone because of the low values of Δn^{σ} that were measured in each dose. The heat output curves changed from a sharp peak in the first doses to a markedly tail-shape on increasing the amount absorbed, in close correlation with the differences observed in adsorption rates. This fact added difficulty in accurately measuring the differential heat of adsorption at the final points of the isotherm. Heats of readsorption were in good agreement with heats of adsorption, provided the coverage was shifted to the right-hand side by

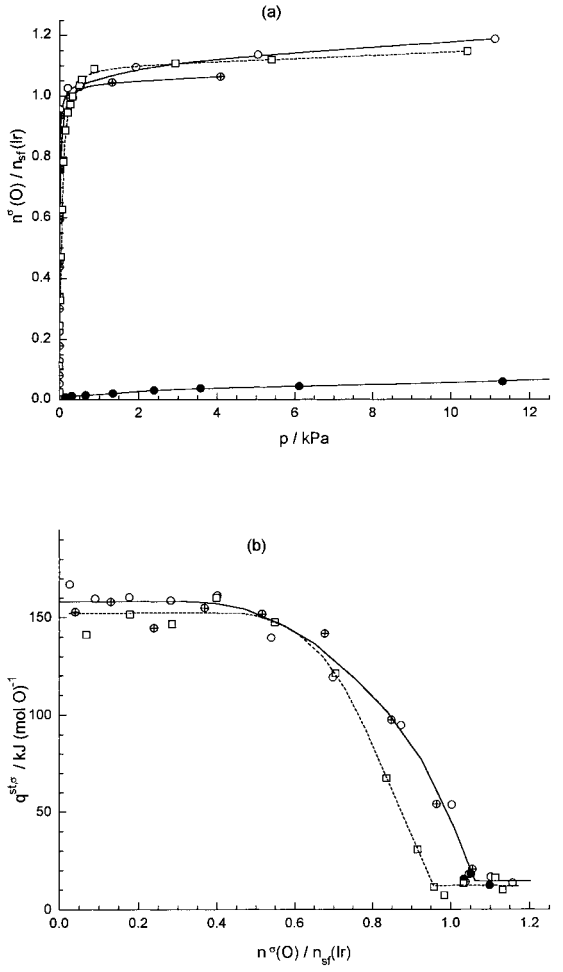

Fig. 3. (a) Volumetric and (b) differential calorimetric isotherms of oxygen adsorption on Ir/SiO_2 samples at 315 K. Samples: 5%, ○ (2 cells), ⊕, ● (1 cell); 0.5%, □ (2 cells). Filled symbols, readsorption experiments.

$n^{\sigma}(H)/n_{sf}(Ir)=0.57$, which is the difference between the two volumetric isotherms.

The *oxygen adsorption* volumetric isotherms on Ir/SiO_2 samples (Fig. 3(a)) are in similar shape to those of hydrogen. Hence, the following con clusions:

1. there occurs a large adsorption at a negligible pressure;
2. there is a knee; and
3. there occurs a slight increase of adsorption at higher pressures.

The adsorption rate in the three regions also showed a similar behaviour: the process was instantaneous in the first region, slow in the knee region, and followed a linear decrease of pressure with time in the final part. The readsorption isotherm was very different from that of hydrogen: there was some oxygen pressure from the first dose, and the isotherm looks like an extension of the final part of the isotherm on the clean sample.

The oxygen differential calorimetric isotherms on Ir/SiO_2 samples (Fig. 3(b)) are very different from those of hydrogen. The adsorption heat remained approximately constant up to nearly half the monolayer, then described a convex curve up to $O^{\sigma}/Ir_{sf}=1.05$, and ended in a plateau of ca. 10–15 kJ (mol O)$^{-1}$. Values of $q^{st,\sigma}$ are much higher than those of hydrogen adsorption. The initial plateau of the O–Ir/SiO_2 0.5% sample was slightly lower than that of the Ir/SiO_2 5% sample. The correlation observed in hydrogen adsorption between differences in the heat-output curves and change of adsorption rate, as successive doses are added, is also noticed here. Moreover, the calorimeter signal of the final doses did not return to the baseline, which is an evidence of the existence of a very slow process that ensues when the experiment was stopped. A few $q^{st,\sigma}$ values of the readsorption isotherm are plotted in Fig. 3(b) in order to confirm that this isotherm is the continuation of the slow process taking place at the end of the adsorption isotherm on the clean sample.

3.2. *Ir/γ-Al_2O_3*

Hydrogen- and oxygen-adsorption volumetric and differential calorimetric isotherms on Ir/γ-Al_2O_3 samples (Figs. 4 and 5) are similar to those on the Ir/SiO_2 samples. Changes in the adsorption rate and heat-output curves, that occurred with silica-supported samples as adsorption progressed, presented similar features in experiments on the alumina-supported samples. Nevertheless, some important differences were manifest.

The hydrogen uptake in the volumetric isotherms (Fig. 4(a)), expressed as H^{σ}/Ir_{sf}, was much higher than that for Ir/SiO_2 catalysts. Moreover, it also changed from unsintered Ir/Al_2O_3 2.5% – 1 samples to sintered 2.5% – 2 ones, no differences being noticed between the two sintered 2.5%–2.1 and 2.5%–2.2 samples.

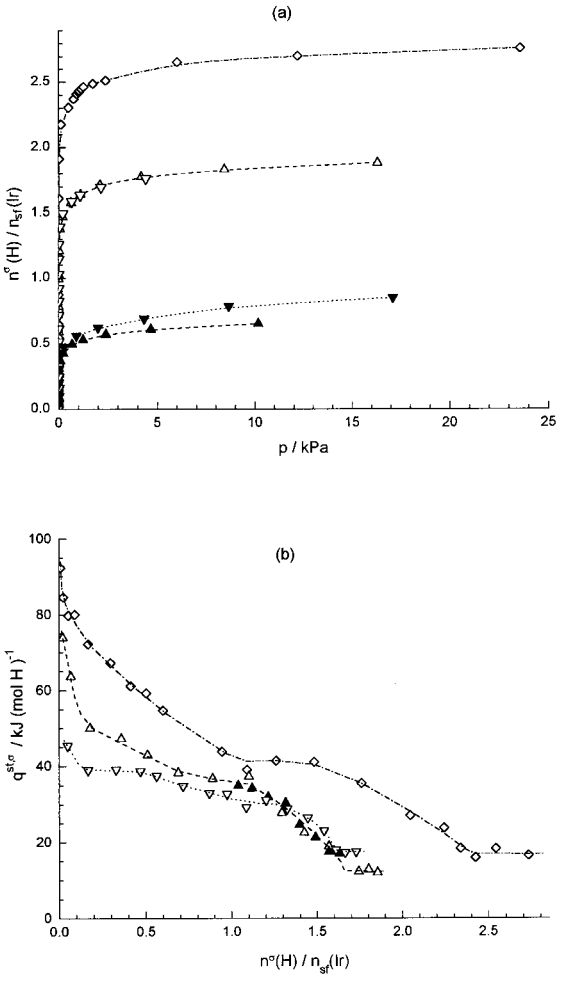

Fig. 4. (a) Volumetric and (b) differential calorimetric isotherms of hydrogen adsorption on Ir/γ-Al_2O_3 samples at 315 K. Samples: 2.5% – 1.1, ◇; 2.5% – 2.1, △,▲; 2.5% – 2.2, ▽,▼. One cell in all cases. Filled symbols represent readsorption experiments.

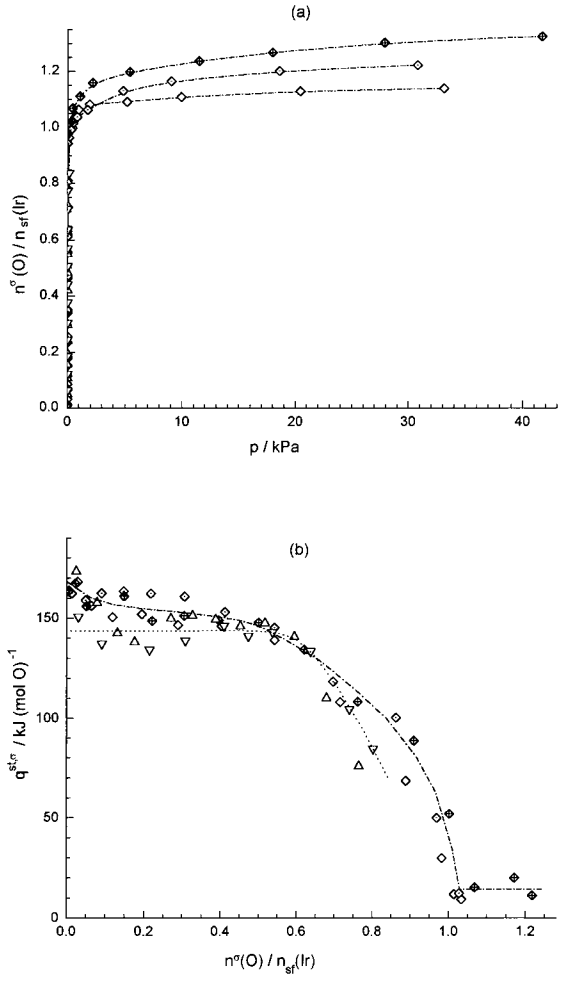

Fig. 5. (a) Volumetric and (b) differential calorimetric isotherms of oxygen adsorption on Ir/γ-Al_2O_3 at 315 K. Samples: 2.5% – 1.1, ◇ (2 cells); 2.5% – 1.2, ◈ (2 cells); ✣ (1 cell); 2.5% – 2.1, △ (1 cell); 2.5% – 2.2, ▽ (1 cell).

Stoichiometries, H^{σ}/Ir_{sf}, were around 2.3–2.5 and 1.5–1.7 on the knee of the unsintered and sintered samples, respectively. The final part of all isotherms run parallel. In readsorption isotherms on the sintered samples the initial vertical region reaches a common value of $H^{\sigma}/Ir_{sf} \approx 0.5$, the same value as in the hydrogen readsorption isotherm on the Ir/SiO_2 5% sample.

Hydrogen differential calorimetric isotherms on the four Ir/Al_2O_3 samples (Fig. 4(b)) show large differences not only in the value of $q^{st,\sigma}$, but also in its dependence on coverage, even between the two sintered samples. The distinct H^{σ}/Ir_{sf} uptakes seen in the volumetric isotherms were also observed. Values as high as 95 kJ (mol H)$^{-1}$ at very low uptakes were measured for the unsintered sample.

At variance, oxygen adsorption isotherms exhibited similar O^{σ}/Ir_{sf} uptakes for all Ir/Al_2O_3 catalysts (Fig. 5(a)); and also similar to those observed on the Ir/SiO_2 samples. A common value of 1.0–1.1 at the isotherm knee is observed.

The corresponding differential calorimetric isotherms (Fig. 5(b)) are also similar, although those corresponding to the most sintered sample, Ir/Al_2O_3 2.5% – 2.2, showed somewhat lower values.

4. Discussion

The common features of all *volumetric isotherms* presented in this work (Fig. 2(a), Fig. 3(a), Fig. 4(a), Fig. 5(a)) indicate that adsorption processes are of the same type:

1. A large initial uptake that took place almost instantaneously at negligible pressures, denotes a strong adsorption. The values of H^{σ}/Ir_{sf} or O^{σ}/Ir_{sf} were near unity, except for hydrogen adsorption on Ir/Al_2O_3 catalysts where values ca. 2.4 and 1.5 were obtained for the 2.5%–1 and 2.5%–2 samples, respectively.
2. In the following isotherm knee, adsorption was slower and some gas remained in the gas phase.
3. A final region, where only slight uptake increases were produced by large pressure increments, corresponds to an activated process that proceeded at a very slow constant rate.

Hydrogen readsorption isotherms can be made to coincide with the corresponding isotherms on the clean sample by displacing them upwards by the irreversibly adsorbed amount existing in each case under the particular experimental conditions. Oxygen readsorption is of a different nature and will be discussed in the following.

On the contrary, the differential calorimetric isotherms were quite different for the various adsorbate/adsorbent systems, revealing important differences among the adsorption processes that were not apparent in the volumetric isotherms.

Hydrogen differential calorimetric isotherms had a similar shape for all the samples (Fig. 2(b), Fig. 4(b)) and can be correlated to the three regions of the volumetric isotherms.

The first region is assigned to adsorption on most of the metal-particle surface, which exhibits a heterogeneous character. Surface mobility of the adsorbed species had to exist in order to ensure the possibility that the most energetic sites be occupied first. An initial abrupt fall of $q^{st,\sigma}$, very short in the H-Ir/SiO_2 experiments, and the step zone that followed up to roughly half the monolayer capacity (Table 2), can be ascribed to adsorption on the most energetic sites: corners, edges, point defects. The following zone of lower slope should correspond to adsorption on crystallite faces. Afterwards, the second region – the isotherm knee – is clearly marked in the calorimetric isotherm by a sudden fall in the adsorption heat. It would drop to zero values, except for the presence of an additional process that produced the final plateau. This abrupt fall clearly indicates completion of the monolayer (Table 2).

The adsorption heat and the hydrogen coverage that define the limits of each region certainly change from one sample to another, as can be observed in Table 2 and Fig. 6(a), that shows $q^{st,\sigma}$-n^{σ} curves fitted to the experimental points for each sample. The adsorption heats are high for the unsintered Ir/Al_2O_3 2.5%–1.1 sample, in which coverage reached 2.4 H atoms per surface Ir atom at monolayer completion. Although the two Ir/Al_2O_3 2.5% – 2 sintered samples had similar H^{σ}/Ir_{sf} stoichiometries, the $q^{st,\sigma}$-n^{σ} curves showed that the adsorption heat was lower, and the homogeneity larger, for the most sintered sample, Ir/Al_2O_3 2.5% – 2.2. Results for the two Ir/SiO_2 samples follow the same $q^{st,\sigma}$-n^{σ} curve in agreement with their similar metal particle sizes (Table 1). Their hydrogen adsorption heats and surface heterogeneities are comparable to those of the Ir/Al_2O_3 2.5% – 2.1 sample, although uptakes were lower.

Table 2
Characteristic uptakes in the hydrogen and oxygen differential calorimetric isotherms [a]

	Ir/SiO_2		Ir/Al_2O_3		
	5%	0.5%	2.5% – 1	2.5% – 2.1	2.5% – 2.2
H slope change [b]	0.5		1.0	0.7	0.6
H monolayer completion	1.10		2.40	1.65	1.60
O monolayer completion	1.05	≈0.95	1.03	≈0.95	≈0.95

[a] Uptakes expressed as $n^{\sigma}(H)/n_{sf}(Ir)$ or $n^{\sigma}(O)/n_{sf}(Ir)$.
[b] Midpoint of the monolayer at which the slope of the hydrogen $q^{st,\sigma}$-n^{σ} curve changes (see text).

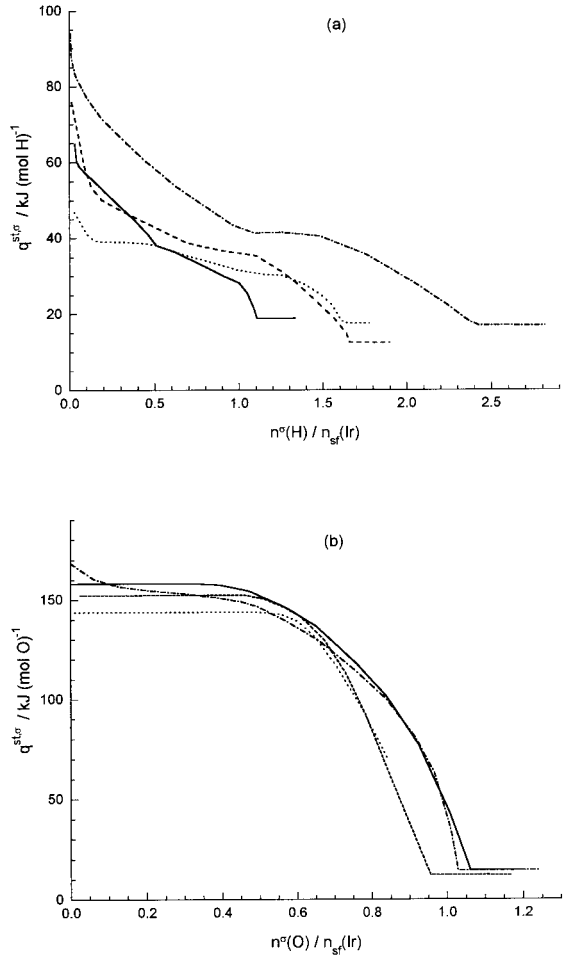

Fig. 6. Comparison of differential calorimetric isotherms of: (a) hydrogen, and (b) oxygen on the different samples. Samples: Ir/SiO_2, (———) 5%; and (- - -) 0.5%. Ir/Al_2O_3, (- · -) 2.5% – 1; (– – –) 2.5% – 2.1; and (· · ·) 2.5% – 2.2.

Previous measurements of the differential heat of adsorption of hydrogen on samples of iridium supported on diverse aluminas also showed values somewhat different for the different samples [22]. They increased as metal dispersion increased. The various $q^{st,\sigma}$-n^{σ} curves are placed closed to those of our sintered samples. Heat values for hydrogen adsorption on a Ir/SiO_2 sample [23] are also somewhat lower than ours. The same happens with a Ir/Grafoil sample [24]. In the latter case, a mean metallic particle size ca. 5–6 nm was measured by various methods. The existence of bigger crystallites may produce a lower heat of adsorption, besides the possible effect of the support being a quite different material from silica or alumina. This explanation can also be applied to the other cases.

The differential calorimetric isotherms of hydrogen readsorption, (Fig. 2(b), Fig. 4(b)), coincide with those on the clean sample if they are shifted to the right by irreversible adsorption as calculated from volumetric results. This proves that the experiment simply consisted in hydrogen readsorption on the same sites that were emptied in the intermediate outgassing.

The third region of the hydrogen $q^{st,\sigma}$–n^{σ} isotherms, occurring after completion of the monolayer, is a plateau with a common value of 17–18 kJ (mol H)$^{-1}$ for all the samples (Fig. 6). The same final plateau, at ca. 12 kJ mol^{-1}, was found in the adsorption of hydrogen on Ir/Grafoil [24]. This process could be identified with weak molecular adsorption on iridium or spillover to the support [25–27]. The spillover hypothesis can be disregarded since adsorption kinetic experiments at higher temperatures did not show a rate increase [17].

Differential calorimetric isotherms of oxygen adsorption were very similar for all the samples (Fig. 3(b), Fig. 5(b)). In the first region of the volumetric isotherm there are two segments: an initial plateau up to $n^{\sigma}(O)/n_{sf}(Ir)\approx 0.5$, with somewhat higher values of $q^{st,\sigma}$ at very low coverages in the O–Ir/Al_2O_3 systems, followed by a convex decrease of the adsorption heat, i.e. with increasing slope as adsorption progressed. Indeed, these oxygen isotherms are very different from the hydrogen isotherms. Since intrinsic heterogeneity of the sample is beyond doubt, we have to postulate that the strength of the O–Ir bond restricted surface mobility, i.e. the oxygen atoms remained on those surface sites where they were first adsorbed. Therefore, a $q^{st,\sigma}$ random mean value is measured for each dose. Moreover, if this assumption is true, the adsorption heat decrease following the plateau cannot be ascribed to the sample intrinsic heterogeneity. A change in the electronic properties of the metal particles induced by the already adsorbed oxygen may be postulated [28]. In fact, calculation of $q^{st,\sigma}$–n^{σ} curves of O–Ir/SiO_2 and O–Ir/Al_2O_3 made from hydrogen-preadsorbed oxygen titration data, only partially published [29], revealed the iridium surface heterogeneity for oxygen adsorption in a completely different picture.

The shape of our oxygen differential calorimetric isotherms is similar to earlier results in respect of Ir/

SiO_2 and Ir/Al_2O_3 [30]. The values of the adsorption heat at the plateau are also analogous. The metal particle size of their samples was comparable to that of our Ir/Al_2O_3 sintered samples. Different behaviour between samples of iridium on different aluminas was found by other workers [22], the effect not being correlated to metal dispersion. The authors associated a decrease of the oxygen adsorption heat to the amount of unreduced iridium as determined by XPS. Results of the two totally reduced samples lay in the same differential calorimetric isotherm which nearly coincides with those of our samples. High differential heats of oxygen adsorption have been measured on a Ir/Grafoil sample [24]. We may speculate that the nature of the support influences the energetics of the oxygen adsorption process.

The region of the knee in the oxygen volumetric isotherm does not show up at the end of the heat decrease. The plateau that follows, with a value of 10–15 kJ (mol O)$^{-1}$, corresponds to the final part (third region) of the volumetric isotherm. The same heat values of the final part were obtained in the oxygen readsorption isotherm (Fig. 3(b)). Therefore, this experiment seems to measure the extent of the final process of the adsorption isotherm. There was no reversible adsorption because of the strong O–Ir bond. The final process can be identified as the formation of some kind of surface oxide in a complex process that involved oxygen already adsorbed and oxygen from the gas phase. It had been detected by XPS and UPS at temperatures >600 K ([31,32], and discussion in Ref. [17]) but it was produced in our experiments at lower temperatures because of the high degree of dispersion of some of the catalyst samples.

Values of $n^{\sigma}(O)/n_{sf}(Ir) \approx 1$ at the completion of the oxygen monolayer (Table 2) confirm the validity of the method used for determining the amount of superficial iridium [17]. They are slightly higher than 1, 1.03–1.05, which may be due to the concurrence with adsorption of some surface oxidation in the last doses. Monolayer completion as seen in the differential calorimetric isotherms on samples Ir/SiO_2 0.5% and Ir/Al_2O_3 2.5% – 2.1 and 2.5% – 2.2 took place at the values somewhat lower than $n^{\sigma}(O)/n_{sf}(Ir)=1$ (Table 2). The discrepancy, ca. 5%, may be attributed to the very low amount of surface iridium on these samples (Table 1), which made the determination of $n_{sf}(Ir)$ less accurate. Since the calorimetric results clearly establish when the monolayer is completed, values of $n_{sf}(Ir)$ in Table 1 should be slightly decreased.

It is interesting to point out that the amount adsorbed at the completion of the monolayer corresponds to the middle of the knee of the volumetric isotherms. This information may be helpful to determine approximate values of the monolayer capacity from a volumetric isotherm when calorimetric data are not available.

Contrary to the hydrogen isotherms, oxygen calorimetric isotherms on all the samples are nearly coincident (Fig. 6(b)). Only those on the sintered samples are lower. We had postulated [17] that the dependence of hydrogen adsorption stoichiometry on support and particle size is related to crystallite size and shape, and to differences in metal–support interaction [17]. It was demonstrated that the H^{σ}/Ir_{sf} ratio increased with increasing dispersion. Stoichiometries $CO^{\sigma}/Ir_{sf} \geq 2$ have been explained by the presence of plate-like particles [33,34]. The same explanation can account for the dependence found here for the heats of the H-Ir/support systems on the support and on the degree of sintering. We can postulate plate-like iridium particles in Ir/Al_2O_3 2.5%–1 samples, which show some metal–support interaction, to explain the very high H^{σ}/Ir_{sf} stoichiometries and strong H–Ir bonding, whereas cubic particles would be present in Ir/SiO_2 5% and 0.5% samples with H^{σ}/Ir_{sf} ratios near 1 and much lower heats of hydrogen adsorption. The sintering process applied to the Ir/Al_2O_3 catalyst would convert the plate-like into cubic particles, lowering the H^{σ}/Ir_{sf} stoichiometry and the H–Ir bond strength to different degrees. If oxygen adsorption takes place at random, as postulated above, then the sample heterogeneity would not show up in oxygen calorimetric experiments. In any case, sample differences that produced changes in H^{σ}/Ir_{sf} stoichiometry and adsorption heat did not produce an analogous effect in oxygen adsorption.

5. Conclusions

Adsorption microcalorimetry has been applied to study the adsorption of hydrogen and oxygen on supported iridium catalysts. Samples of Ir/SiO_2 and Ir/Al_2O_3 of different metallic particle sizes were used.

Hydrogen adsorption stoichiometries higher than one at monolayer completion were confirmed. The

lowest value, 1.1, corresponded to Ir/SiO_2 samples, the highest one, 2.4, pertained to the most dispersed Ir/Al_2O_3 samples, and values ca. 1.6 were found for sintered Ir/Al_2O_3 samples. Plots of differential heat of adsorption vs. amount adsorbed revealed the intrinsic heterogeneity of all the samples, its decrease with increasing degree of sintering being certainly observed. The heat depended on support and particle size, following the same trend as did stoichiometries.

On the contrary, oxygen adsorption stoichiometries and heat vs. coverage curves were very similar for all samples. The shape of the differential calorimetric isotherms induced us to postulate as follows:

(i) immobility of oxygen surface species caused by a very strong O–Ir bond; and
(ii) change of metal crystallite electronic properties as adsorption proceeded, due to the oxygen already adsorbed.

The dependence of hydrogen adsorption stoichiometry and heat values on support and on particle size may be related to crystallite size and shape, and to differences in metal–support interaction. On the contrary, oxygen adsorption features in all samples were similar. The completion of the monolayer is clearly identified in the differential calorimetric isotherms, $q^{st,\sigma}$ vs. n^{σ}. The amount of adsorbed oxygen at this point practically coincided with the amount of superficial iridium, determined by the already reported volumetric method [17].

The final process that continued when the experiment was stopped is ascribed to weak adsorption in the case of hydrogen, spillover to the support being unlikely, and to surface oxidation in the case of oxygen isotherms.

Acknowledgements

This work was partially supported by the DGICYT, Spanish Ministry of Education and Science, under Project No. PB94-0006-CO2

References

[1] K. Foger, J.R. Anderson, J. Catal. 59 (1979) 325.
[2] A.G. Burden, J.G. Grant, J. Martos, R.B. Moyes, P.B. Wells, Faraday Disc. Chem. Soc. 72 (1981) 95.
[3] S. Taniguchi, T. Mori, Y. Mori, T. Hattori, Y. Murakami, J. Catal. 116 (1989) 108.
[4] K. Nakagawa, T. Suzuki, T. Kobayashi, M. Haruta, Chem. Lett. (1996) 1029.
[5] M.F. Mark, W.F. Maier, J. Catal. 164 (1996) 122.
[6] C.G. Walter, B. Coq, F. Figueras, M. Boulet, Appl. Catal. A Gen. 133 (1995) 95.
[7] A. Zhao, B.C. Gates, J. Amer. Chem. Soc. 118 (1996) 2458.
[8] L. Basini, A. Aragno, G. Vlaic, Catal. Lett. 39 (1996) 49.
[9] A. Erdohelyi, K. Fodor, G. Suru, Appl. Catal. A Gen. 139 (1996) 131.
[10] J.C. Rasser, W.H. Beindorf, J.J.F. Scholten, J. Catal. 59 (1979) 211.
[11] M.J. Dees, V. Ponec, J. Catal. 115 (1989) 347.
[12] M. Ogura, E. Kikuchi, Chem. Lett. (1996) 1017.
[13] D. Kelly, W.H. Weinberg, J. Chem. Phys. 105 (1996) 271, 7171 and 11313.
[14] D.C. Seets, M.C. Wheeler, C.B. Mullins, Chem. Phys. Lett. 266 (1997) 431.
[15] N.D. Triantafillou, S.E. Deutsch, O. Alexeev, J.T. Miller, B.C. Gates, J. Catal. 159 (1996) 14.
[16] M. Cabrejas Manchado, J.M. Guil, A. Ruiz Paniego, J. Chem. Soc., Faraday Trans. 1, 85 (1989) 1775.
[17] M. Cabrejas Manchado, J.M. Guil, A. Ruiz Paniego, J. Catal. 136 (1992) 598.
[18] D.H. Everett, Pure Appl. Chem. 31 (1972) 579.
[19] J.M. Guil, A. Pérez Masiá, A. Ruiz Paniego, J.M. Trejo Menayo, J. Chem. Thermodyn. 26 (1994) 5.
[20] M. Cabrejas Manchado, J.M. Guil, A. Pérez Masiá, A. Ruiz Paniego, J.M. Trejo Menayo, Langmuir 10 (1994) 685.
[21] N. Cardona-Martinez, J.A. Dumesic, Adv. Catal. 38 (1992) 149.
[22] Yu.D. Pankratiev, N.E. Buyanova, V.M. Turkov, A.P. Shepelin, E.M. Malyshev, P.A. Zhdan, React. Kinet. Catal. Lett. 20 (1982) 139.
[23] S.A. Goddard, M.D. Amiridis, J.E. Rekoske, N. Cardona-Martinez, J.A. Dumesic, J. Catal. 117 (1989) 155.
[24] J. Cobes, J. Phillips, J. Phys. Chem. 95 (1991) 8776; 95 (1991) 5545.
[25] G.M. Panjonk, S.J. Teichner, J.E. Germain (Eds.), Spillover of Adsorbed Species, Elsevier Sci. Pub., Amsterdam, 1983.
[26] J.J.F. Scholten, An. Quim., 81 (1985) 475 and 485.
[27] B.J. Kip, F.B.M. Duivenvoorden, D.C. Koningsberger, R. Prins, J. Catal. 105 (1987) 26.
[28] J.M. Rojo, J.P. Belzunegui, J. Sanz, J.M. Guil, J. Phys. Chem. 98 (1994) 13631.
[29] J.M. Guil, A.P. Masiá, A.R. Paniego, J.M.T. Menayo, Stud. Surf. Sci. Catal. 75 (1993) 1859.
[30] G.D. Zakumbaeva, V.A. Naidin, A.M. Dostiyarov, B.B. Dyusenbina, React. Kinet. Catal. Lett. 19 (1982) 303.
[31] P.A. Zhdan, G.K. Boreskov, A.I. Boronin, W.F. Egelhoff, W.H. Weinberg, Surf. Sci. 61 (1976) 25.
[32] H. Conrad, J. Kuppers, F. Nitschke, A. Plagge, Surf. Sci. 69 (1977) 668.
[33] J.R. Anderson, P.S. Elmes, R.F. Howe, D.E. Mainwaring, J. Catal. 50 (1977) 508.
[34] K. Tanaka, K.L. Watters, R.F. Howe, J. Catal. 75 (1982) 23.